JOURNAL OF SOLID STATE CHEMISTRY 108, 267–274 (1994)

Crystal Structure and Magnetic Properties of $BaVSi_2O_7$

Guo Liu and J. E. Greedan[1]

Institute for Materials Research, McMaster University, Hamilton, Ontario, Canada L8S 4M1

Received February 1, 1993; accepted May 28, 1993

The structure of the second phase (β-) of $BaVSi_2O_7$ has been solved by single crystal X-ray diffraction, and its magnetic properties have been examined in the temperature range 5–300 K. β-$BaVSi_2O_7$ crystallizes in the tetragonal system, space group $I4/m$ (No. 87), with $a = 7.0535(7)$ Å, $c = 11.467(2)$, $V = 570.5(3)$ Å^3, and $Z = 4$. This structure can be considered as consisting of VO_5^{6-} square pyramids and unbranched single rings of $[Si_4O_{12}]^{8-}$, or of cage-like $[Si_4V_2O_{18}]^{12-}$ clusters formed by SiO_4^{4-} and VO_5^{6-}. These building elements are cross-linked to form a pseudo-two-dimensional (2D) network containing empty channels perpendicular to the c-axis. The 2D networks are held together by Ba^{2+} ions that occupy channels parallel to the c-axis. β-$BaVSi_2O_7$ undergoes short range magnetic order below ~20 K. Its behavior can best be described as an $S = \frac{1}{2}$ dimer with $J/k = -19.0$ K, $\bar{g} = 1.87$. The fresnoite-type $Ba_2VSi_2O_8$ is found to be a Curie–Weiss paramagnet down to 4.5 K.

INTRODUCTION

Tetravalent vanadium is known to form silicates with some alkaline earth elements (Ca, Sr, and Ba) where V(IV) adopts square pyramidal (VO_5^{6-}) coordination and Si is tetrahedrally coordinated (1–3). Feltz and co-workers (4) first reported the synthesis of $Ba_2VSi_2O_8$ and $BaVSi_2O_7$, and showed that the former appeared to be isostructural with the tetragonal fresnoite $Ba_2TiSi_2O_8$, in which TiO_5^{6-} square pyramids and $Si_2O_7^{6-}$ dimers are linked to form a layered structure (5–7). Two polymorphs have been reported for $BaVSi_2O_7$. The recently discovered mineral suzukiite (3), (α-) $BaVSi_2O_7$, was said to have the haradaite ($SrVSi_2O_7$) structure, in which VO_5^{6-} square pyramids and $[Si_4O_{12}]_n$ chains are cross-linked to form again a layered structure (2). The second form, β) $BaVSi_2O_7$, was thought to be orthorhombic (4) (and probably isostructural with $BaTiSi_2O_7$) based on powder X-ray diffraction data, but detailed crystallographic information was not available. During our investigation in the $BaVO_{3-x}$ system, we accidently obtained good quality single crystals of β-$BaVSi_2O_7$, and less well crystallized $Ba_2VSi_2O_8$. Thus we carried out a structure determination of β-$BaVSi_2O_7$ by single crystal X-ray diffraction, and examined the magnetic properties of both V(IV)-containing silicates.

[1] To whom correspondence should be addressed.

EXPERIMENTAL

Sample Preparation

Synthesis of $Ba_8V_7O_{22}$. $Ba_2V_2O_7$ was first synthesized by firing an intimate mixture of $2BaCO_3$ and V_2O_5 at 900–1000°C in air. $Ba_2V_2O_7$ powder specimens were reduced in flowing H_2 gas at 1100°C for 24 hr. The dark gray product was ground further, pelleted, confined in an open Mo tube (O.D. 1.25 cm) which was secured in an alumina boat, heated in H_2 at 1350°C for 2–4 days depending on the sample size, and cooled down rapidly. The pellet surface near both ends of the Mo tube was partially reoxidized (white), probably during cooling; the white material was removed physically. The structure of the major product has been solved by single crystal X-ray diffraction recently and its composition established as $Ba_8V_7O_{22}$, in which V exhibits three oxidation states (+3, +4, and +5) (8).

Crystal growth of β-$BaVSi_2O_7$. A mixture of $Ba_8V_7O_{22}$ (0.167 g, ~9% by weight) and $BaCl_2$ (1.788 g) was loaded into a clean quartz tube, evacuated to 10^{-4} Torr with mild heating (below 100°C) to completely remove water absorbed by $BaCl_2$, and sealed off. The quartz tube was heated at 6–10°C/min to 1020°C, soaked for 30 min, and cooled at 6°C/hr to 850°C, then at 20°C/hr to 500°C, and finally, rapidly, to room temperature. The product was washed repeatedly with distilled water to remove the flux. Well crystallized greenish transparent thin plate crystals were easily picked out from the bulk powder specimen. As described below, the powder X-ray diffraction pattern matched that of $BaVSi_2O_7$ reported previously (4), for which $Z = 4$ had been derived from the measured density. The composition is proved by single crystal X-ray structure analysis.

Crystal growth of $Ba_2VSi_2O_8$. A mixture of $Ba_8V_7O_{22}$ (0.245 g, ~18% by weight) and $BaCl_2$ (1.153 g) was treated

0022-4596/94 $6.00

in the same way as for β-$BaVSi_2O_7$ in quartz, but was cooled at 20°C/hr to 600°C, and then rapidly to room temperature. Colorless square rod crystals were found when the product was washed repeatedly with distilled water. The surfaces of most crystals were covered with black materials which had to be removed by washing and scratching. No efforts were made to improve the quality of the crystals. Powder X-ray diffraction proved this to be the same phase as $Ba_2VSi_2O_8$ reported previously (4).

Powder X-Ray Diffraction and Magnetic Measurements

Preliminary examinations were performed using a Guinier–Hägg camera (IRDAB XDC700) with Cu$K\alpha$1 radiation and a Si standard. Pulverized crystals were mounted on Scotch tape for Guinier photography. The Guinier data were read with a computer-controlled automated LS-20 type line scanner (KEJ Instruments, Täby, Sweden). Susceptibility data were obtained using a Quantum Design SQUID magnetometer in the temperature range 4.5–300 K using ~10 mg randomly oriented crystals at an applied magnetic field of 0.2 T. Diamagnetic corrections were applied.

Single Crystal X-Ray Structure Analysis of β-$BaVSi_2O_7$

A thin plate crystal was mounted on the tip of a glass fiber with epoxy cement and examined on a Siemens P3 four-circle diffractometer using Ag$K\alpha$ radiation. Three standards ((4 0 0); (0 4 0); (0 0 4)), measured at every 100 reflections, showed no measurable decay in intensity. Data reduction, structure solution, and refinement were effected using the Siemens SHELXTL PC software package on an IBM-compatible 80486 personal computer. Seven azimuthal scans ((0 k 0) where k = 2, 4, 6, 8, 10, 12, 14) were used for absorption corrections using the program XEMP based on a lamina model with (0 0 1) for the prominent face of the thin plate crystal. Systematic extinction conditions (hkl: $h + k + l \neq 2n$) and intensity statistics suggested that the most likely space group is the centrosymmetric $I4/m$ (#87), which has been determined in the subsequent refinement. Atomic coordinates of all the heavy atoms, Ba, V, and Si, were found by direct methods, and the oxygens were located by Fourier difference. The structural and anisotropic thermal parameters were refined by full least-squares methods based on $(F_o - F_c)^2$ using 904 observed reflections with $I_o > 3\sigma(I_o)$ to R = 4.75%, R_w = 7.17% and GOF = 1.96. Detailed crystallographic information is listed in Table 1. The noncentrosymmetric space group $I\bar{4}$ was also tested. The reliability factors were slightly lower (R = 4.13%, R_w = 5.73%, and GOF = 1.62) due to the increase in refinable parameters. However, strong correlations between certain parameter pairs, high shift/error ratios, and the appearance of unreasonably short O · · · O contact distances (2.425 Å) are clear indications of an improper choice of space group. Therefore the space group $I\bar{4}$ was rejected for β-$BaVSi_2O_7$.

TABLE 1
Summary of Crystallographic Data for β-$BaVSi_2O_7$

Color and habit	Greenish, thin plate
Crystal size (mm^3)	0.21 × 0.19 × 0.023
Diffractometer	Siemens P3
Radiation	Ag$K\alpha$(λ = 0.56086 Å)
Temperature (K)	290
Monochromator	Graphite
2θ range (°)	6.0 to 70.0
Index ranges	$-1 \leq h \leq 14$, $-1 < k \leq 14$, $-1 \leq l \leq 23$
Scan type	ω
Scan speed (°/min.)	Variable; 2.00 to 29.30 in ω
Scan range (ω, °)	0.06
Absorption correction	Semi-empirical
Min./max. transmission	0.5117/0.8661
Crystal system	Tetragonal
Systematic extinction conditions	hkl: $h + k + l \neq 2n$
Space group	$I4/m$
Unit cell dimensions (Å)	a = 7.0535(7) c = 11.467(2)
Volume ($Å^3$)	570.5(3)
Z	4
Formula weight	356.5
Density (calc., g/cm^3)	4.150
Absorption coefficient (mm^{-1})	8.903
F(000)	652
No. of reflections collected	1747
No. of independent reflections	1280
No. of observed reflections	904 ($F_o^2 > 3\sigma(F_o^2)$)
No. of parameters refined	31
Data/parameter ratio	29.2
R(%)	4.75
R_w(%)	7.17
Goodness-of-fit	1.96
Largest shift/error, Δ/σ	0.003

RESULTS AND DISCUSSION

The Crystal Structure of β-$BaVSi_2O_7$

Atomic coordinates and isotropic temperature factors are listed in Table 2, anistropic temperature factors in Table 3, and important bond lengths and bond angles in Table 4. As can be seen in Fig. 1, the structure consists of unbranched single $[Si_4O_{12}]^{8-}$ rings and VO_5^{6-} square pyramids. The $[Si_4O_{12}]^{8-}$ group has a C_{4h} symmetry as shown more clearly in Fig. 2, while the VO_5^{6-} group has a lower (C_{4v}) symmetry. The Si–O bond lengths range from 1.597(5) to 1.622(5) Å (average 1.606(5) Å), and

TABLE 2
Atomic Coordinates and Equivalent Isotropic Displacement Coefficients ($Å^2 \times 10^3$) for β-$BaVSi_2O_7$

Atom	Site	x	y	z	U(eq)
Ba	4*d*	0.5000	0	0.2500	16(1)
V	4*e*	0	0	0.3433(1)	7(1)
Si	8*h*	0.2313(2)	0.2175(2)	0	11(1)
O(1)	8*h*	0.2650(8)	−0.0099(7)	0	30(2)
O(2)	16*i*	0.1783(7)	0.1986(8)	0.3826(4)	35(1)
O(3)	4*e*	0	0	0.2044(7)	26(2)

Note. Equivalent isotropic u defined as one third of the trace of the orthogonalized U_{ij} tensor.

O–Si–O angles from 107.9(2)° to 114.2(4)° (average 109.5(3)°). These results are in good agreement with existing silicates (9), and suggest a relatively small distortion from a regular tetrahedron. Similar $[Si_4O_{12}]^{8-}$ rings have been observed in a few other silicates such as M'–Pb_2SiO_4 (10), the leucosphenite $Na_4BaTi_2B_2Si_{10}O_{30}$ (11), and taramellite $Ba_4M_4(B_2Si_8O_{27})O_2Cl_x$ (M = Ti^{4+}, Fe^{3+}; $0 \le x \le 1$) (12). In the VO_5^{6-} square pyramid, the axial V–O bond length is only 1.592(8) Å, while the basal ones are significantly longer, 1.936(5) Å. The O(2)–V–O(3) basal to axial oxygen angle, 103.5(1)°, is greater than 90° and clearly indicates the displacement of the central V atom off the basal square plane toward the axial oxygen. This geometry is similar to the VO_5^{6-} polyhedra in the haradaite $SrVSi_2O_7$(2), cavansite, and pentagonite (Ca(VO)(Si_4O_{10})·$4H_2O$) (1), and to the MV_3O_7 series (M = Ca, Sr, Cd) (13). The VO_5^{6-} polyhedra are isolated in the sense that there is no direct connection between themselves. However, they can be considered as dimerized through four bridging Si atoms, forming a $[Si_4V_2O_{18}]^{12-}$ cluster as shown in Fig. 3 (C_{4h} symmetry).

The cross linking of SiO_4^{4-} and VO_5^{6-} polyhedra results in the formation of a two-dimensional channel structure as shown in Fig. 4. It consists of 8-membered rings involving

TABLE 3
Anisotropic Displacement Coefficients ($Å^2 \times 10^3$) for β-$BaVSi_2O_7$

Atom	U_{11}	U_{22}	U_{33}	U_{12}	U_{13}	U_{23}
Ba	16(1)	16(1)	15(1)	0	0	0
V	8(1)	8(1)	7(1)	0	0	0
Si	10(1)	9(1)	13(1)	−7(1)	0	0
O(1)	12(2)	13(2)	66(5)	−1(1)	0	0
O(2)	35(2)	50(3)	22(2)	−33(2)	−7(2)	−2(2)
O(3)	36(3)	36(3)	5(2)	0	0	0

Note. The anisotropic displacement exponent takes the form $-2\pi^2(h^2a^{*2}U_{11} + \cdots + 2hka^*b^*U_{12})$.

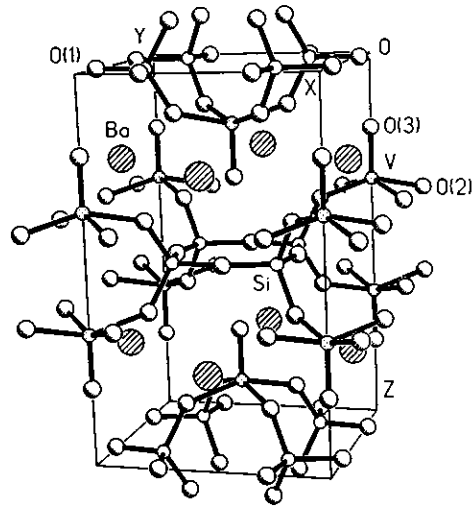

FIG. 1. The β-$BaVSi_2O_7$ structure with SiO_4^{4-} and VO_5^{6-} polyhedra outlined.

both Si and V as well as O atoms. The V · · · V distance in Fig. 3, 3.594 Å, sets an upper limit for the channel height. The 2D channel structure of β-$BaVSi_2O_7$ is unique among the known V(IV)- and Ti(IV)-containing silicates. Though in the fresnoite structure of $Ba_2TiSi_2O_8$ (7) and $Ba_2VSi_2O_8$ (4), and the haradaite structure of $SrVSi_2O_7$

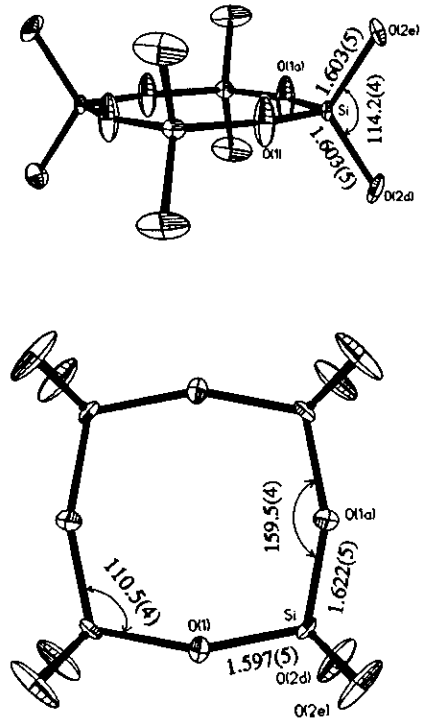

FIG. 2. Side and top views of an unbranched single $[Si_4O_{12}]^{8-}$ ring (C_{4h} symmetry). Bond lengths (Å) and important bond angles (°) are also given. Atoms are plotted at 50% probability level.

TABLE 4
Important Bond Lengths (Å) and Bond Angles (°) for β-$BaVSi_2O_7$

		BaO_n			
	4 Ba–O(1)		3.312(3)		
	4 Ba–O(2)		3.070(5)		
	4 Ba–O(2)′		2.901(5)		
	4 Ba–O(3)		3.566(1)		
	Average	12x	3.094(4)		
	Ba–O	16x	3.212(3)		
	VO_5			SiO_4	
V–O(3)	1.592(8)		Si–O(1)	1.622(5)	
4 V–O(2)	1.936(5)		Si–O(1)′	1.597(5)	
Average	1.867(6)		2 Si–O(2)	1.603(5)	
			Average	1.606(5)	
4 O(2)–V–O(3)	103.5(1)		O(1)–Si–O(1)′	110.5(4)	
2 O(2)–V–O(2)′	153.0(3)		2 O(1)–Si–O(2)′	107.9(2)	
4 O(2)–V–O(2)″	86.9(1)		2 O(1)′–Si–O(2)′	108.2(2)	
			O(2)–Si–(2)′	114.2(4)	
			Average	109.5(3)	
2 O(1)–Ba	3.312(3)		O(2)–Ba	2.901(5)	
O(1)–Si	1.597(5)		O(2)–Ba′	3.070(5)	
O(1)–Si′	1.622(5)		2 O(2)–Si	1.603(5)	
O(3)–V	1.592(8)				
4 O(3)–Ba	3.566(1)				
	Shortest O ··· O		2.592		

(2) and $BaVSi_2O_7$ (suzukiite) (3), the SiO_4^{4-} and VO_5^{6-} TiO_5^{6-}) polyhedra form layers which are held together by Ba^{2+} or Sr^{2+} ions, they do not have the open channels found in the β-$BaVSi_2O_7$ structure. However, β-$BaVSi_2O_7$ is not believed to be as zeolitic as cavansite and pentagonite (1), where large 16- and 12-membered rings involving only Si and O atoms have been found, respectively.

The coordination of the Ba^{2+} ions that hold the 2D networks together in β-$BaVSi_2O_7$ is worthy of a close examination. They occupy channels parallel to the c-axis as can be seen more clearly from a perspective view along the c-axis in Fig. 5. Within the sphere of a 3.5 Å radius the Ba^{2+} ions can be considered as 12-coordinated with Ba–O bond lengths ranging from 2.901(5) to 3.312(3) Å and an average of 3.094(4) Å. If the four additional oxygens at a distance of 3.566(1) Å were considered, the Ba^{2+} ions would be 16-coordinated with an even longer average Ba–O distance (3.212(3) Å). The average Ba–O distance for the 12-coordination is already larger than that in the fresnoite $Ba_2TiSi_2O_8$ (average Ba–O 2.98(3) Å) and those in Ba_2VO_4 (2.883(15); 3.042(16) Å) (14). These results suggest that the Ba^{2+} ions are rather weakly bonded in β-$BaVSi_2O_7$.

Finally it is worth commenting on the highly anistropic thermal parameters of O(1) and O(3). As can be seen in Table 3, there exist significant differences between the U_{11}, U_{22}, and U_{33} components for both oxygens. Since thermal motions are related to bonding, these results appear to reflect the special coordination environments of O(1) and O(3). O(3) is strongly bonded to one V with the V–O bond parallel to the c-axis, and much more weakly to four Ba^{2+} as described above. Thus thermal motion in

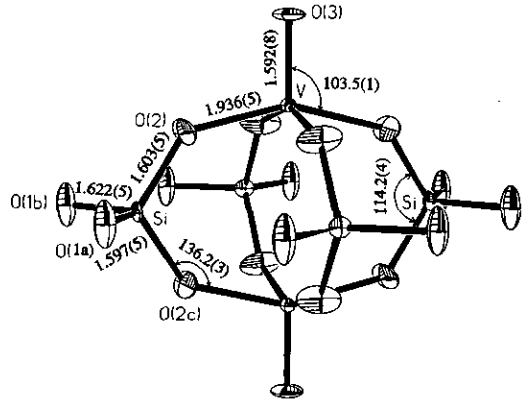

FIG. 3. A $[Si_4V_2O_{18}]^{12-}$ cluster (C_{4h} symmetry) showing the dimerization of the VO_5^{6-} square pyramids. Atoms are plotted at 50% probability level.

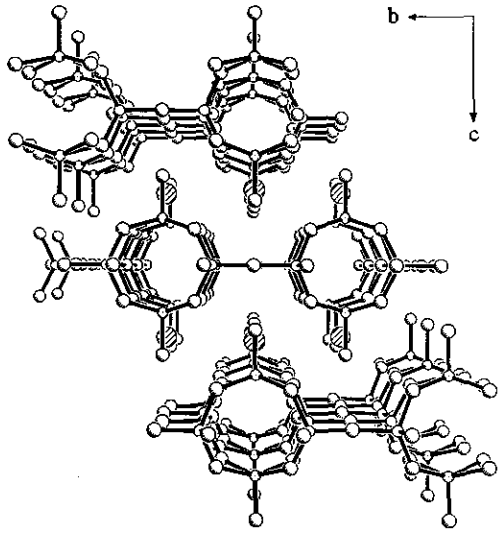

FIG. 4. Perspective view of the β-$BaVSi_2O_7$ structure alone the a-axis showing the existence of 2D networks and empty channels perpendicular to the c-axis.

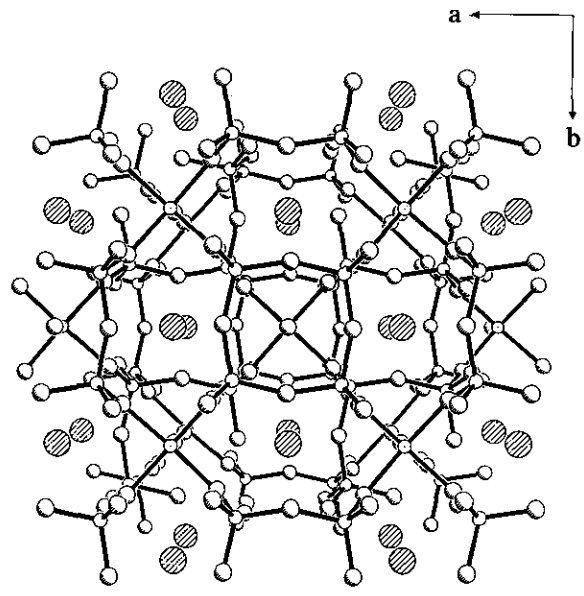

FIG. 5. Perspective view of the β-$BaVSi_2O_7$ structure alone the c-axis showing the occupation of channels by Ba^{2+} ions (shaded large circles) parallel to the c-axis.

the Z direction is very small as is the U_{33} value with respect to U_{11} and U_{22}. O(1), on the other hand, forms a quite irregular tetrahedron. It is loosely bonded to two Ba (Ba–O(1): 3.312(3) Å) with the Ba–O(1)–Ba (119.9(2)°) at ~30° with respect to the c-axis, while rather tightly to two Si (Si–O(1): 1.597(5), 1.621(5) Å and Si–O(1)–Si 159.4(4)°) in a plane perpendicular to the c-axis. Therefore, the U_{33} component of O(1) is significantly higher than U_{11} and U_{22}.

Powder X-ray Diffraction

β-$BaVSi_2O_7$. Twenty observed reflections from Guinier X-ray data were indexed by the program TREOR90P, a PC version of TREOR (15), to the tetragonal system, with a = 7.0506(3), c = 11.4643(7) Å, and V = 569.89 Å^3 and figures of merit M20 = 54, F20 = 60. The least-squares refined cell parameters using 38 unique reflections are listed in Table 5, together with related V(IV) and Ti(IV) silicates for comparison. The observed powder X-ray diffraction pattern is listed in Table 6. The powder pattern appears to be identical with the graphically shown pattern of "orthorhombic" $BaVSi_2O_7$ reported by Feltz and coworkers (4), and the two solutions have similar unit cell volumes (Table 5). Thus they probably represent the same phase.

$Ba_2VSi_2O_8$. Twenty-two observed reflections were indexed completely by TREOR90P to the tetragonal system (M22 = 72, F22 = 63), with a = 8.5015(6), c = 5.2158(6) Å, and V = 376.98 Å^3. The least-squares refined cell pa-

TABLE 5
Comparison of Observed Lattice Parameters for Some V(IV)- and Ti(IV)-Containing Silicates

Compound	Space group	a(Å)	b(Å)	c(Å)	V(Å)	Reference
$BaVSi_2O_7$	*I*4/m	7.0507(3)		11.4665(7)	570.02(5)	This work
$BaVSi_2O_7$		6.01(2)	10.00(4)	9.55(4)	574(5)	(4)
$BaVSi_2O_7$	*Ama*2	7.089(2)	15.261(2)	5.364(1)	580.3	(3)
$SrVSi_2O_7$	*Amam*	7.06	14.64	5.33	551	(2)
$Ba_2VSi_2O_8$	*P*4*bm*	8.5017(4)		5.2145(4)	376.90(4)	This work
$Ba_2VSi_2O_8$	*P*4*bm*	8.488(8)		5.210(5)	375.5	(4)
$Ba_2TiSi_2O_8$	*P*4*bm*	8.5291		5.2110	379.08	(16)

TABLE 6
Guinier X-Ray Diffraction Pattern of Pulverized $BaVSi_2O_7$ Crystals

h	k	l	d_{cal}	d_{obs}	I_{obs}
1	0	1	6.006	6.014	4
0	0	2	5.7332	5.7330	4
1	1	0	4.9858	4.9892	14
1	1	2	3.7621	3.7643	27
2	0	0	3.5253	3.5270	16
1	0	3	3.3609	3.3612	15
2	1	1	3.0403	3.0405	10
2	0	2	3.0030	3.0043	100
0	0	4	2.8666	2.8668	4
2	2	0	2.4928	2.4932	60
1	1	4	2.4851	2.4854	24
2	2	2	2.2861	2.2864	24
3	1	0	2.2296	2.2299	10
2	0	4	2.2241	2.2241	5
1	0	5	2.1808	2.1801	2
3	1	2	2.0780	2.0781	14
2	2	4	1.8810	1.8804	5
1	1	6	1.7845	1.7845	9
4	0	0	1.7627	1.7624	49
3	2	3	1.7409	1.7412	5
4	0	2	1.6848	1.6847	4
2	0	6	1.6801	1.6798	5
3	3	2	1.5962	1.5959	9
4	2	0	1.5766	1.5767	15
4	1	3	1.5609	1.5608	3
4	2	2	1.5201	1.5203	29
4	0	4	1.5015	1.5013	8
3	2	5	1.4880	1.4880	2
3	1	6	1.4510	1.4509	11
3	3	4	1.4377	1.4373	23
0	0	8	1.4333	1.4330	3
1	1	8	1.3775	1.3777	3
5	1	2	1.3442	1.3443	6
4	3	3	1.3230	1.3231	3
5	2	1	1.3008	1.3006	3
3	3	6	1.2540	1.2542	5
2	2	8	1.2426	1.2426	4
4	2	6	1.2161	1.2168	5
5	3	0	1.2092	1.2086	2
3	1	8	1.2057	1.2059	7

Note. $\lambda = 1.5406$ Å, $a = 7.0507(3)$ Å, $c = 11.4665(7)$ Å, $\overline{V} = 570.02(5)$ Å^3; $I4/m$.

rameters using 26 unique reflections are also listed in Table 5. The unit cell is slightly larger than that reported previously for $Ba_2VSi_2O_8$, but smaller than the fresnoite $Ba_2TiSi_2O_8$. The observed powder pattern is listed in Table 7. This pattern is so similar to that of $Ba_2TiSi_2O_8$ (16) that it is clear that the crystals obtained in this experiment are $Ba_2VSi_2O_8$, and the compound has the fresnoite structure as suggested previously (4).

TABLE 7
Guinier X-Ray Diffraction Pattern of $Ba_2VSi_2O_8$

h	k	l	d_{cal}	d_{obs}	I_{obs}
0	0	1	5.215	5.211	6
2	0	0	4.251	4.258	3
1	1	1	3.9391	3.9387	9
2	1	0	3.8021	3.7995	19
2	0	1	3.2948	3.2942	41
2	1	1	3.0722	3.0720	100
2	2	0	3.0058	3.0057	6
3	1	0	2.6885	2.6882	34
0	0	2	2.6072	2.6071	19
3	1	1	2.3896	2.3897	9
2	0	2	2.2225	2.2231	8
2	1	2	2.1502	2.1507	23
4	1	0	2.0620	2.0614	31
3	3	0	2.0039	2.0040	14
2	2	2	1.9696	1.9697	9
4	2	0	1.9010	1.9006	6
3	3	1	1.8705	1.8707	30
4	1	2	1.6173	1.6177	11
3	3	2	1.5888	1.5886	16
2	1	3	1.5808	1.5811	14
5	2	1	1.5110	1.5112	16
6	0	0	1.4170	1.4169	6
5	3	1	1.4042	1.4038	6
4	1	3	1.3290	1.3292	11
6	2	1	1.3017	1.3018	11
5	4	1	1.2867	1.2868	6
1	1	4	1.2740	1.2737	6

Note. $\lambda = 1.5406$ Å, $a = 8.5017(4)$ Å, $c = 5.2145(4)$ Å, $V = 376.90(4)$ Å^3; space group $P4bm$.

Magnetic Properties

β-$BaVSi_2O_7$. The magnetic susceptibility and inverse susceptibility data are plotted against temperature in Fig. 6. There exists a relatively broad susceptibility maximum

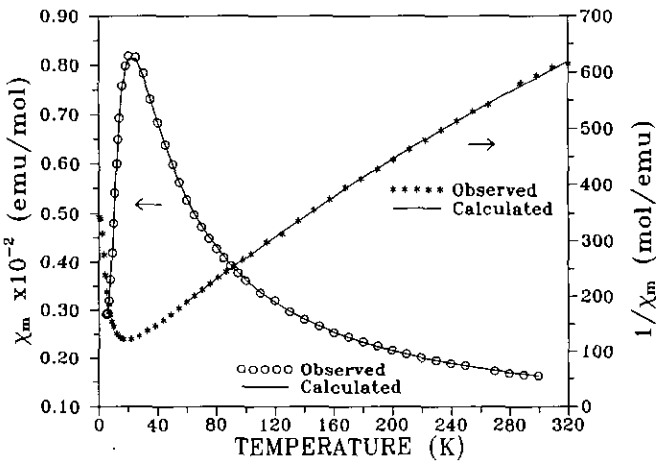

FIG. 6. Temperature dependencies of the magnetic susceptibility per V (left) and inverse susceptibility (right) of β-$BaVSi_2O_7$. Calculated curves are based on an $S = \frac{1}{2}$ dimer (left) and the Curie–Weiss law (right).

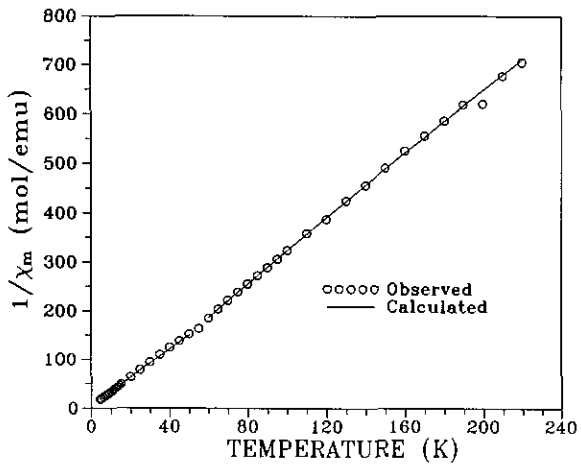

FIG. 7. Temperature dependence of the inverse susceptibility of $Ba_2VSi_2O_8$ with Curie–Weiss law fits in two different temperature ranges.

at ~22 K, indicating short-range magnetic order. Efforts to correlate the observed susceptibility data quantitatively to a short-range model showed that the best fit can be obtained for an $S = \frac{1}{2}$ dimer. The equation used for the fitting can be written as

$$\chi_m = \frac{N\bar{g}^2\mu_B^2}{3kT}\left[1 + \left(\frac{1}{3}\right)\exp(-2J/kT)\right]^{-1} + \frac{C}{T-\theta} + \chi_{TIP} \qquad [1]$$

where $\bar{g}$ is the powder-averaged g-factor, and J the exchange constant. The first term is the Bleaney–Bowers expression (17) per V atom for an $S = \frac{1}{2}$ dimer system, the second (Curie–Weiss law) term accounts for the trace amount of paramagnetic impurity whose contribution was only observable at ~6 K, and the last term accounts for temperature-independent paramagnetism. As can be seen in Fig. 6, this equation gave an excellent fit to the observed data with $J/k = -19.0$ K, $\bar{g} = 1.87$, $\chi_{TIP} = 4.97 \times 10^{-4}$ emu/mol, $C = 0.0212$ emu · K/mol, and $\theta = -4.2$ K.

The dimeric antiferromagnetic interaction can be understood by examining the cluster structure shown in Fig. 3. This mechanism involves superexchange through the four O–Si–O bridges. Relevant bond lengths and bond angles for such a V–O(2)–Si–O(2)′–V′ bridge are, from left to right: 1.936(5) Å, 1.603(5), 1.603(5), 1.936(5); 136.2(3)°, 114.2(4)°, 136.2(3)°. Such a pathway should allow good orbital overlaps which are important for the superexchange interaction. Also, this pathway should be favored over that which would result in two-dimensional correlations, namely, V–O(2)–Si–O(1)–Si′–O(2)′–V′ (Fig. 1).

We recently reported another magnetic dimer for V(IV) in the high temperature (β-) phase of Sr_2VO_4 (18), where the formation of a somewhat loosely defined chemical dimer, $V_2O_8^{8-}$, has been observed (14). The magnetic coupling is much stronger in β-Sr_2VO_4 ($\bar{g} = 1.88$, $J/k = -52$ K) than in β-$BaVSi_2O_7$ despite the involvement of a long V–O bond (2.37 Å) in the superexchange pathway in the former case. Thus it is believed that the V–O–V bond angle, 147°, played a crucial role in the magnetic exchange in β-Sr_2VO_4, while in β-$BaVSi_2O_7$ the relatively small exchange coupling constant is probably due to the combined effects of smaller bond angles and the presence of an additional atom, Si, in the superexchange pathway.

TABLE 8
Observed and Ideal Bond Valence Sums (V) for the Crystallographically Independent Atoms in β-$BaVSi_2O_7$

Atom	Ba	V	Si	O(1)	O(2)	O(3)
V(obs.)	1.61	4.33	4.38	−2.30	−2.08	−1.80
V(ideal)	2	4	4	−2	−2	−2

The inverse susceptibility curve in the temperature range 60–300 K can be fitted to a Curie–Weiss law with a temperature-independent term. This gave $C = 0.374$ emu · K/mol, which is exactly that expected for an $S = \frac{1}{2}$ spin-only system ($C = 0.375$ emu · K/mol) for V(IV), $\theta = -17.4$ K, and $\chi_{TIP} = 4.37 \times 10^{-4}$ emu/mol, which is close to the value in the dimer model fitting.

$Ba_2VSi_2O_8$. The temperature dependence of the inverse susceptibility data is plotted in Fig. 7. A Curie–Weiss law is observed down to 4.5 K. There appears to be a change in slope at ~55 K; its origin is unknown. A fitting to the data in the 60–220 K range gave $C = 0.271$ emu · K/mol, $\theta = 8.2$ K, and $\chi_{TIP} = 1.26 \times 10^{-4}$ emu/mol. The low temperature data between 4.5 and 50 K gave $\theta = -1.7$ K and $C = 0.344$ emu · K/mol, which is close to the spin-only value of 0.375 emu · K/mol.

Bond Valence Sums

A bond valence sum, V, for a given ion is defined as the sum of bond valences (s_i) of its individual bonds according to the equation

$$V = \Sigma s_i = \Sigma \exp[(r_o - r_i)/B], \qquad [2]$$

where r_i is the observed bond length for the ith bond, and B and r_o are semiempirical parameters which have been calculated by Brown and Altermatt (19). V can be used to describe the distribution of valence in bonds, and is normally expected to be close to the oxidation state of the ion concerned. An increase in V represents a shortening of bonds and a decrease in V means a lengthening of bonds. Derived bond valence sums from known bond lengths for β-$BaVSi_2O_7$ are listed in Table 8. Apparently, the V, Si,

and O(1) atoms are tightly bonded because of their importance in the formation of the $[Si_4O_{12}]^{8-}$ rings and $[Si_4V_2O_{18}]^{12-}$ clusters, while the Ba atoms, which fill the channels as described above, are rather loosely bonded. The small bond valence sum for O(3), however, cannot be interpreted simply as a result of bond stretching because of its unusual coordination environment. The O(3)–Ba bonds are lengthened indeed, while the bond valence value of −1.80 for the axial O(3)–V bond is a very high value, and reflects the strong double bond nature of V–O(3).

ACKNOWLEDGMENT

We thank Dr. J. Britten for assistance in the single crystal X-ray diffraction work and Professor C. V. Stager for use of the magnetometer. The financial support of the Natural Science and Engineering Research Council of Canada and the Ontario Centre for Materials Research are acknowledged gratefully.

REFERENCES

1. H. T. Evans, Jr., *Am. Mineral.* **58,** 412 (1973).
2. Y. Takeuchi and W. Joswig, *Mineral. J.* **5,** 98 (1967).
3. S. Matsubara, A. Kato, and S. Yui, *Mineral. J.* **11,** 15 (1982).
4. A. Feltz, S. Schmalfuss, H. Langbein, and M. Tietz, *Z. Anorg. Allg. Chem.* **417,** 125 (1975).
5. R. Masse, J.-C. Grenier, and A. Durif, *Bull. Soc. Fr. Minér. Crist.* **90,** 20 (1967).
6. P. B. Moore and J. Louisnathan, *Science* **156,** 1361 (1967).
7. P. B. Moore and S. J. Louisnathan, *Z. Kristallogr.* **130,** 438 (1969).
8. G. Liu and J. E. Greedan, *J. Solid State Chem.*, in press.
9. F. Liebau, "Structural Chemistry of Silicates: Structure, Bonding, and Classification," Springer-Verlag, Berlin/New York, 1985.
10. L. S. Dent Glasser, R. A. Howie, and R. M. Smart, *Acta Crystallogr. Sect. B* **37,** 303 (1981).
11. Yu. A. Malinovskii, N. A. Yamnova, and A. N. V. Belov, *Sov. Phys. Dokl.* **26,** 372 (1981).
12. F. Mazzi and G. Rossi, *Am. Mineral.* **65,** 123 (1980).
13. G. Liu and J. E. Greedan, *J. Solid State Chem.* **103,** 139 (1993).
14. G. Liu and J. E. Greedan, *J. Solid State Chem.* **103,** 228 (1993).
15. P. E. Werner, L. Eriksson, and M. Westdahl, *J. Appl. Crystallogr.* **18,** 367 (1985).
16. Powder Diffraction File card 22-513, JCPDS: International Centre for Diffraction Data, 1601 Park Lane, Swarthmore, PA 19081.
17. B. Bleaney and K. D. Bowers, *Proc. R. Soc. London Ser. A* **214,** 451 (1952).
18. W. Gong, J. E. Greedan, G. Liu, and M. Bjorgvinsson, *J. Solid State Chem.* **95,** 213 (1991).
19. I. D. Brown and D. Altermatt, *Acta Crystallogr. Sect. B* **41,** 244 (1985).